A Review on Preprocessing and Segmentation Techniques in Carotid Artery Ultrasound Images

K. V. Archana and R. Vanithamani

Abstract Epidemiological studies reveal that anatomical changes of carotid artery due to deposition of fatty lesions are effective signs of cardiovascular diseases. Ultrasound imaging modality provides the cross-sectional view of these arteries to identify the deposited plaques. Segmentation of common carotid artery (CCA) wall is important in determining the thickness of intima-media region of carotid artery. With the development of automated systems in medical field, a plethora of algorithms and strategies to analyze the carotid artery are proposed by various researchers over a period. This review focus on the techniques that have been developed for preprocessing and segmentation of various parts of the carotid artery from the longitudinal B-mode ultrasound images using both automated and semi-automated techniques. The review ends with a discussion about the techniques and future perspectives to make the computer-based carotid artery analysis more accurate and reliable.

Keywords Common Carotid Artery · Longitudinal ultrasound images · Despeckle · Segmentation

1 Introduction

Over the past decade, a rise of 26.6% of cardiovascular cases is noted. According to the experts of [1], the long-term effects of COVID-19 are likely to influence cardiovascular health, and the global burden of cardiovascular disease is expected to grow exponentially over the next few years. The pathological mechanism of cardiovascular

K. V. Archana (✉)
Department of Electronics and Communication Engineering, School of Engineering, Avinashilingam Institute for Home Science and Higher Education for Women, Coimbatore, Tamil Nadu, India
e-mail: archana_ece@avinuty.ac.in

R. Vanithamani
Department of Biomedical Instrumentation Engineering, School of Engineering, Avinashilingam Institute for Home Science and Higher Education for Women, Coimbatore, Tamil Nadu, India
e-mail: vanithamani_bmie@avinuty.ac.in

V. Suma et al. (eds.), *Evolutionary Computing and Mobile Sustainable Networks*,
Lecture Notes on Data Engineering and Communications Technologies 116,
https://doi.org/10.1007/978-981-16-9605-3_62

diseases starts with deposition of lipoprotein cholesterol, thickening of vessel walls, increased degrees of vascularization, and formation of atherosclerotic plague on the vessel walls [2]. Figure 1a represents a longitudinal B-mode ultrasound image of the carotid artery, and Fig. 1b depicts a plague region in carotid artery. This plague can break off from the inner walls of the blood vessels and enter the circulation causing arterial obstruction. This stimulates thrombus or vasospasm in heart, brain, kidneys, and lower extremities [3–5].

Precise imaging of the common carotid artery is important for diagnosis as well as assessing the risk of various vascular diseases. There are various imaging modalities used for this purpose, namely ultrasound, invasive coronary angiography, and Magnetic Resonance Imaging (MRI). Angiography is a routine procedure to locate the plague or affected area, but it does not provide structural information [6]. Ultrasonography is the preferred method of vascular imaging due to its reliability, low cost, non-invasiveness, and better visualization of anatomical structures. Important quantitative information such as lumen area, thickness of the carotid walls, distribution and composition of plaques, and intima-media thickness are available in longitudinal ultrasound images [7]. Therefore, analysis of the arterial wall and plague deposits in coronary artery has significant clinical relevance for assessment and management of cardiovascular diseases. Conventionally, these details are measured from ultrasound images by trained personals in clinical setting which is highly user-dependent, time-consuming, and prone to errors. Due to the advent of automation, several computerized techniques have been developed to reduce the subjectivity and time of analysis while increasing the accuracy and efficiency. A large number of follow-up studies have been done on B-mode ultrasound images to determine the possibilities of carotid atherosclerosis or stenosis [3, 8, 9]. A cohort study in [10] reveals that diabetic patient along with renal dysfunction are more susceptible to carotid stenosis leading to mortality.

Since the ultrasound image acquisition procedure is completely manual, the parameter settings of the machine depend on the subjective judgment of the operator. Thus, the acquisition of good quality ultrasound images is complicated and requires

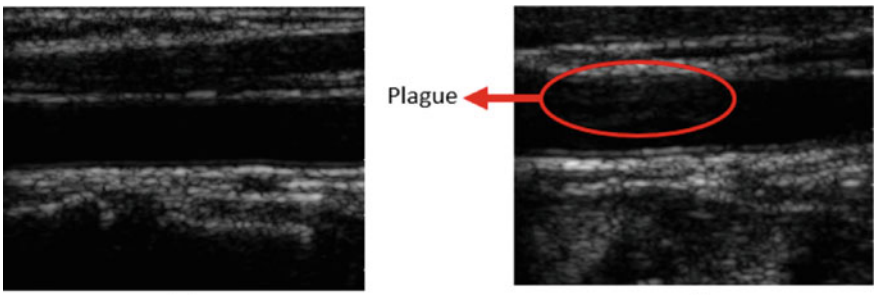

Fig. 1 Longitudinal B-mode ultrasound image of carotid artery: **a** healthy, **b** plague deposits on the arterial wall

high skilled personal. Regardless of the acquisition protocols, the echogenicity depends on tissue composition, insonation angle, tissue attenuation, and blood flow. This leads to local changes in intensity, contrast, and adds speckle pattern in ultrasound images. Hence, particular attention should be given to suppress the speckle pattern before segmentation. The intention of this article is to give an extensive appraisal on the analysis of carotid artery ultrasound images for disease diagnosis starting from image denoising for speckle reduction and segmentation approaches.

2 Preprocessing

Due to ultrasonic echoes from tissues, ultrasound images are often accompanied by multiplying speckle noise. This falsifies the fine details of the image, making it difficult for the computer system to analyze the information. Therefore, despeckling of ultrasound images is critical for better diagnosis of pathologies. Several speckle reduction techniques have been proposed, especially for ultrasound B-mode images. Table.1 shows some of the speckle reduction techniques considered in this study. Commonly available despeckling filters are mean, Lee, Kuan, Wiener, and Gaussian filters. Speckle reducing anisotropic diffusion (SRAD) filter developed by [11] is a benchmark filter for despeckling [12, 13]. Filtering in wavelet domain has also gained popularity among researchers [12, 14]. Linear scaling filter and local statistical filter that utilizes mean and variance are also applied to despeckle the image [15–17]. Whereas, authors of [13] developed an integrated toolbox in MATLAB that includes ten despeckling filters specially utilized for carotid artery ultrasound images. On contrary, multiplicative noise is converted into additive noise in [18] and applied wavelet decomposition. Then, three different filters, namely non-local means (NLM), vectorial total variation (VTV), and block matching and 3D filtering (BM3D) algorithms are applied. Whereas, utilized non-local variational model is used in [19] for despeckling of ultrasound images. Table 1 shows the comparative analysis of the despeckling algorithm that are implemented and the performance metrics used for analysis.

3 Segmentation

This section highlights the state-of-the art techniques that facilitate segmentation of carotid artery from longitudinal ultrasound images and are listed in Table 2. Researchers developed different methodologies such as edge detection methods, thresholding methods, contours or snakes, and classifier-based approaches.

Thresholding Simple thresholding methods like Otsu thresholding using wind-driven optimization, global thresholding followed by morphological operations are

Table 1 Despeckling techniques implemented for longitudinal B-mode carotid artery ultrasound images

Name, Year, and Ref. No.	Despeckling techniques	Features extracted for analysis	Advantages and limitations
Loizou et al. 2007 [20, 21]	Linear scaling mean variance	Mean and variance	• Image normalization prior to speckle reduction • Improved image quality
Izquierdo-Zaragoza et al. 2011 [22]	Low pass Gaussian filter, morphological filtering	–	• Clean the image highlighting only the relevant information
Petroudi et al. 2012 [15]	Speckle removal linear scaling filter	Local mean and variance	• Edge preservation is better • No comparison with other despeckling filters
Ramasamy and Jayanthi 2013 [23]	Gaussian filter	–	• The smoothing effect reduces the impact of noise in the image • Alters the position of the object boundaries for increased radius
Chaudhry et al. 2013 [24]	Median filter	–	• Smooth out noise and preserves image details in better way compared to average and bilateral filters
Loizou et al. 2014 [13]	(a) Linear filter, (b) Wiener linear filter, (c) linear filter, (d) Nonlinear filter, (e) Geometric filter, (f) Median filter, (g) Hybrid median filter, (h) Anisotropic diffusion filter, (i) Coherent nonlinear anisotropic diffusion filter, (j) SRAD	Statistical features, spatial gray-level dependence matrices, gray-level difference statistics, neighborhood gray tone difference matrix, neighborhood gray tone difference matrix, laws texture energy measures, fractal dimension texture analysis, Fourier power spectrum, shape parameters	• Developed a freeware despeckle filtering toolbox which also supports image normalization, delineation of structures, texture extraction • Filters can be applied over entire image as well as in ROI. Validated the performance for IVUS images • Filter parameters are made default. Cannot be configured by user which limits their applications over other medical images • Processing time of the proposed method is high

(continued)

Table 1 (continued)

Name, Year, and Ref. No.	Despeckling techniques	Features extracted for analysis	Advantages and limitations
Nagaraj et al. 2018 [14]	Wiener filtering in wavelet domain	–	• Smoothens the edges still preserving the edge information • Faster ROI extraction • Reduced execution time
Nagaraj et al. 2018 [25]	Optimized Bayesian non-local means filter	–	• Filter suppresses the multiplicative noise by utilizing optimally tuned parameters of grayscale images
Gupta et al. 2018 [17]	Local statistics mean variance filter	Mean, standard deviation, mean square error, quality index, peak signal-to-noise ratio, structural similarity index, correlation coefficient, edge preserving index	• Noise reduction without much loss of information • High similarity index
Latha and Dhanalakshmi 2019 [18]	Calculus approach: • Convert the multiplicative speckle noise into additive • Wavelet decomposition • Three different filters: (a) NLM, (b) VTV, and (c) block matching and BM3D	Peak signal-to-noise ratio, mean square error, mean absolute error, root mean square error, structural similarity, quality factor, correlation, and image enhancement factor	• Preserving edge features to a great extent and better denoising • Noise in high frequency content is removed by identifying the dependent components of the image
Febin and Jidesh 2021 [19]	Non-local variational model	Entropy, equivalent number of looks, natural image quality evaluator, global contrast factor, contrast-to-noise ratio	• Despeckling with contrast enhancement and illumination correction • Retaining fine texture details • Less execution time
Latha et al. 2021 [26]	Curvelet decomposition with smooth edge and sparsity	–	• Best denoised results and also reserves maximum of the necessary edge features • Smoothens low frequency noise and the oscillatory high frequency noise are filtered

Table 2 Segmentation techniques implemented for longitudinal B-mode carotid artery ultrasound images

Reference No.	No. of images	Technique	Performance metrics	Merits and demerits
[12]	–	Modified Otsu threshold	–	• Low computational complexity • Better edge detection • Algorithm is unstable for the images with changes in morphological structure of carotid artery
[25]	90	Otsu thresholding using wind-driven optimization	CC, CoV	• Better boundary estimation compared to model based and snake segmentation • No significant deviation between the automated and the ground truth data measurement
[23]	50	Global thresholding + Hole filling	–	• Excellent in quantifying the elasticity and stiffness of carotid artery • No classification made between health and unhealthy subjects
[16, 27]	20	Edge detection using Prewitt operator Edge detection—global threshold + Sobel operator, Hough transform	Error –	• Better speckle noise reduction • Effective detection of inner edges of artery wall • IMT measurement with less error • İmplemented for minimum dataset
[28]	287	Watershed algorithm	RoC	• Automatic system for identification and discrimination of plaques and non-plaques • Reduced false detection • Minimum number of sample dataset is taken for analysis

(continued)

Table 2 (continued)

Reference No.	No. of images	Technique	Performance metrics	Merits and demerits
[15]	100	Active contours	MAD, HD, PD	• Fully automatic system providing lower absolute mean IMT Error • Aids in evaluation of early stages of atherosclerosis • Does not work appreciably for images with artery wall irregularities
[24]	250	Active contour	–	• Automatic snake initialization using image registration technique • Precise selection of control points for image registration • Plaque characterization is poor
[30]	84	Active oblongs	DI, JI, Se, Sp, Acc, L	• Segmentation accuracy is 97.5% • Segmentation and initialization of luminal wall are done subsequently • Not all performance metrics are compared with the existing techniques
[22]	–	B-spline active contour	Mean, max, min	• Automatic segmentation of arterial wall with contrast enhancement • B-spline provides smooth edges by removing the rough texture in ultrasound images • No automatic initialization of snakes • Validation with more number image set is required to be done

(continued)

Table 2 (continued)

Reference No.	No. of images	Technique	Performance metrics	Merits and demerits
[26]	361	Affinity propagation + DBSCAN, GVF snake model, PSO clustering	JI, DI, HI, RI VoI, Ck, C	• Computation is less time-consuming • Full automatic with no need to initiation of ROI • Suitable for differently oriented carotid images • Proposed algorithm occupies more memory and is computationally marginally costly
[34]	153	(i) $H\infty$ grayscale-derivative constraint snake algorithm; (ii) Kalman snake method, (iii) snake method; (iv) dynamic programming; (v) level set method using Chan-Vese energy functional	MAE	• Minimizes worst case error • Grayscale constrain will automatically correct the position of snake along the ROI • Algorithms segments are better even for images with blurred flocculent structure • The parameters for filter and grayscale contours are selected empirically • Method maintains a fixed shape for IM border which is not optimal when the IM border changes during the sequencing
[37]	30	Mixtures of Nakagami distributions and stochastic optimization	GoF	• Semi-automatic method of segmentation with minimal mean difference from the experts' views • Echogenicity of the tissue is verified well • High computational time

(continued)

Table 2 (continued)

Reference No.	No. of images	Technique	Performance metrics	Merits and demerits
[39]	200	Dynamic programming	Acc, Ct	• Algorithm can selectively detect the object boundary with desired patterns • Robustness and high accuracy in edge detection with minimal computational time • Limitation in plaque identification
[40]	47	Dynamic programming, smooth intensity thresholding surfaces and geometric snakes	–	• Accurate segmentation of arterial wall even for arteries with large, hypo-echogenic or irregular plaques • Detection of luminal wall is difficult with poor quality images
[41]	29	Classifiers (linear SVM, SVM + radial bias function, AdaBoost, random forest)	Se, Sp, DSC overlap, HD EArea, PPD, AEArea	• Auto-context model is improving the accuracy of segmentation making the method more robust and stable • Limited number of images • Not efficient in plaque characterization • High training time
[43]	90,000 image patches	• CNN (patch-based approach)	median, mean, SD, min, max, Sp, Se	Good correlation between estimated output and experts view Though training time is high, testing is achieved in near real-time limited dataset

utilized in [23, 25]. In [12], modified Otsu thresholding followed by morphological operations is used to segment upper and lower walls.

Edge detection methods Usually, the blood tissue interface at the walls of blood vessels gives rise to typical edge patterns. These clearly manifest as borders due to discontinuities in the intensity values and reduced edge reflections. Hence, edge detection methods like Prewitt and Sobel operators followed by Hough transform for segmentation are used [16, 27]. Whereas, gradient filter is applied to detect the edges in image followed by watershed algorithm to segment the lesion in ultrasound images [28]. A drawback of this method is over segmentation leading to false detections which is avoided by cluster analysis.

Snake or contours A variety of snake models are used by researchers in which some are fully automated and some need human intervention for contour initiation. Snake or contour models are edge-based models, wherein the initial contour attracts toward local maxima in the edge map, where the shape of the snake is governed by energy functions. In [15], the boundaries of blood vessels are identified by Chan-Vese level set algorithm which provides excellent initialization for segmentation. The intima-media complex is segmented using active contours as in [21]. Whereas, authors of [29] defined two masks as initial contours for Chan-Vese segmentation of carotid artery walls as well as its bifurcation. The obtained contours are smoothed by cubic spline interpolation and projecting contour points toward local regression line. Active oblongs are utilized in [30] to segment the carotid artery. Hough transform is used to automatically initialize the active oblong in the arterial region followed by pixel offset operations and growing the oblong. The growth of the oblong is optimized using gradient descent technique and Green's theorem. A similar approach using active oblong with five degrees of freedom is proposed by [31] and added a post-processing step (median filter, the canny edge operator, and the cubic curve fitting) to provide a smooth curved area. In [22], a semi-automatic approach using two frequency implemented B-spline snakes is implemented. In addition, a small gravity force is added to the upper contour, and a take-off force to the lower contour to make sure the contours does not remain motionless. Recently, [26] compared three methods to segment lumen area, namely combining affinity propagation and (DBSCAN) density-based spatial clustering of applications with noise, gradient vector flow (GVF) snake model, and particle swarm optimization clustering-based segmentation. The combination of affinity propagation and DBSCAN outperformed the other models with low computational power. Moreover, the outliers were removed by Z-score method. A limitation of contour-based segmentation is the initialization of contour or snakes. To overcome this problem [24, 32], proposed an intelligent algorithm that locates arterial wall areas to set the initial contour, thus making the system fully automated. Jin et al. [33] proposed fully automated algorithm for region identification, contour initialization, and segmentation of intima-lumen and media-adventia layers using general snake and GVF snake. Authors of [34] proposed H∞ grayscale-derivative constraint snake algorithm to segment intima-media borders and compared with the following models: Kalman snake method, snake method, dynamic programming, and level set method using Chan-Vese energy functional. The layers segmented by $H\infty$

algorithm are precisely defined and robust to system error. The performance of four different snake models (Williams and Shah, Lai and Chin, Balloon, and GVF snake) with manual segmentation is compared [20]. Lai and Chin snake model depicted slightly better region of curve than the other models.

Nakagami models Nakagami distributions are considerably used in image processing applications as it provides information about the spatial arrangement and statistical distribution of ultrasound imaging data [35, 36]. An iterative method using mixtures of Nakagami distributions and stochastic optimization is applied in [37]. Moreover in [38], they applied Bayesian segmentation approach modeled by mixtures of three Nakagami distributions. Authors have stated that this kind of segmentation approach is semi-computerized and no longer sensitive to the degree of stenosis or calcification. In addition, these images are not preprocessed due to the fact that the application of filter affects the statistics of data.

Dynamic models Some authors proposed dynamic approach in segmentation. In [39], a combination of dual line detection with edge maps of two edge detectors and coupled snake model is used to maintain parallelism in the intima-media segmentation. Whereas in [40], best fit for cubic spline is searched to identify the adventitia layer. Dynamic programming is employed to segment the lumen boundary. Since dynamic programming causes irregularities in boundaries, a combination of smooth intensity thresholding and hybrid Chan-Vese model is applied as post-processing step.

Other approaches Simple iterative clustering algorithm was used in [41] to produce super pixels of ultrasound image and RealAdaBoost is utilized to produce classification map. A learning-based algorithm extracted the plague region from the classification map. They segmented the plague region using classifiers such as linear support vector machine (SVM), AdaBoost, random forest, and SVM + radial bias function by considering each pixel in the image as features belonging to either normal or plague area. Additionally, auto-context model is implemented with ten iterations. It was found that random forest is superior, and the context features help to stabilize the model. Whereas, [42] proposed multiclass framework using k-means classifier and proved its superior performance with manual tracings. Conversely, convolutional neural network is used to characterize the plague composition using patch-based approach [43]. In paper [44], an integrated graph model and Markov random fields is used to segment the plague region in coronary artery. Whereas, researchers in [45] suggested segmentation of coronary artery using clustering algorithms. They have utilized fuzzy c-means clustering, spatial fuzzy c-means, modified spatial fuzzy c-means, k-means clustering, and self-organizing maps. K-means and self-organizing maps yielded similar results. Furthermore, equal weightage problem has been overcome by modified spatial fuzzy c-means segmentation. Authors of [42] combined scale space paradigm with a boundary-based approach using level sets, while some used level set method without re-initialization with uniform length [46].

The performance metrics used for comparison of segmentation techniques are as follows: mean, max, min, error, relative error, standard deviation (SD), mean

absolute distance (MAD), mean absolute error (MAE), Hausdorff distance (HD), point-to-point distance (PPD), polyline distance (PD), Jaccard index (JI), dice index (DI), Rand index (RI), variation of information (VoI), Cohens kappa (Ck), cophenet (C), sensitivity (Se), specificity (Sp), DSC overlap, EArea, AEArea, point-to-point distance (PPD), Daviea Bouldin index (DBI), partition coefficient (PC), classification entropy (CE), accuracy (Acc), localization (L), true-positive fraction (TPF), and false-positive fraction (FPF), true-negative fraction (TNF), false-negative fraction (FNF), similarity kappa index (KI), and the overlap index (OI), confidence interval (CI), correlation coefficient (CC), coefficient of variation (CoV), percent statistics (PS), goodness-of-fit (GoF), mean contour distance (MCD), computation time (Ct), region of curve (RoC), precision of merit (PoM).

4 Discussion and Conclusion

Several advancements in the field of ultrasonic imaging have been proposed; however, a number of factors hinder automated analysis and disease diagnosis. On analyzing the despeckling approaches, it is evident that some approaches suffer from degraded spatial resolution and increased system complexity. Some techniques face limitations as follows: the window size of filters affects the resultant image quality; hence, a fair choice of window size is necessary; inability to preserve the edges may lead to loss of information; post-processing becomes necessary in some cases.

Whereas, segmentation techniques also had some complications. Boundary-based methods are prone to errors as they are sensitive to gradient variations at the edges [42]. Some authors assumed the arterial structures as straight lines, which is not true in all cases. This has led to false estimation in some scenarios. It is observed that most authors are interested in utilizing contours or snakes for segmentation, but still, they possess some drawbacks such as vulnerable to discontinuities and false edges. Some integrated and dynamic approaches were proposed to overcome these drawbacks. After segmentation, most articles had calculated the characteristics of plague region or thickness of boundary walls which helps in further analysis.

A plethora of techniques has been discussed in this paper. Although better results have been reported, a direct comparison cannot be made due to the following reasons (i) image set used is not same; (ii) some required manual intervention which may introduce human specific errors in final outcome, (iii) different areas of carotid artery (far-end wall, near-end wall, plague, intima-media complex, lumen boundary) are segmented; (iv) some approaches are user-independent, and others were semi-automated. In this context, it is obvious that there is still room for improvement in segmenting carotid artery for real-time diagnosis. Some studies have disclosed that these pathologies may manifest either chronically or acutely in all arterial territories. Hence, a growing interest in vascular imaging and computational analysis helps to expand the diagnostic abilities. Articles like [47, 48] reveal smaller artery size is reported in India, as compared to other western regions of the world due to genetics and lifestyle. Some interpret smaller diameter of arteries in women than men. These

conditions are not taken into account in any of the methods. Hence, future works in automated analysis of carotid artery should consider these anatomical differences for better results.

References

1. Information on https://www.news-medical.net/news/20210127/COVID-19-will-impact-cardiovascular-disease-deaths-for-years-to-come-warn-experts.aspx
2. Insull, W., Jr.: The pathology of atherosclerosis: plaque development and plaque responses to medical treatment. Am. J. Med. **122**, S3–S14 (2009)
3. Steinl, D.C., Kaufmann, B.A.: Ultrasound imaging for risk assessment in atherosclerosis. Int. J. Mol. Sci. **16**(5), 9749–9769 (2015)
4. Cattaneo, M., Wyttenbach, R., Corti, R., Staub, D., Gallino, A.: The growing field of imaging of atherosclerosis in peripheral arteries. Angiology **70**(1), 20–34 (2019)
5. Oikonomou, E., Latsios, G., Vogiatzi, G., Tousoulis, D.: Atherosclerotic Plaque. Coronary Artery Disease, Elsevier, pp. 31–41 (2018)
6. Qiu, W., et al.: An open system for intravascular ultrasound imaging. IEEE Trans. Ultrason. Ferroelectr. Freq. Control **59**(10), 2201–2209 (2012)
7. Sidhu, P.S.: Ultrasound of the carotid and vertebral arteries. Br. Med. Bull. **56**(2), 346–366 (2020)
8. Kastelein, J.J.P., de Groot, E.: Ultrasound imaging techniques for the evaluation of cardiovascular therapies. Eur. Heart J. **29**(7), 849–858 (2008)
9. Liguori, C., Paolillo, A., Pietrosanto, A.: An automatic measurement system for the evaluation of carotid intima-media thickness. IEEE Trans. Instrum. Measure. **50**(6), 1684–1691 (2001)
10. Koroleva, E.A., Khapaev, R.S.: The prevalence and risk factors of carotid artery stenosis in type 2 diabetic patients. In: 2020 Cognitive Sciences, Genomics and Bioinformatics (CSGB) (2020)
11. Yu, Y., Acton, S.T.: Speckle reducing anisotropic diffusion. IEEE Trans. Image Process. **11**, 1260–1270 (2002)
12. Nithya, A., Kayalvizhi, R.: Measurement of lower and upper IMT from ultrasound video frames. Biomed. Pharmacol. J. **8**, 355–364 (2015)
13. Loizou, C.P., Theofanous, C., Pantziaris, M., Kasparis, T.: Despeckle filtering software toolbox for ultrasound imaging of the common carotid artery. Comput. Methods Programs Biomed. **114**(1), 109–124 (2014)
14. Nagaraj, Y., Asha, C.S., Teja, H.S., Narasimhadhan, A.V.: Carotid wall segmentation in longitudinal ultrasound images using structured random forest. Comput. Electr. Eng. **69**, 753–767 (2018)
15. Petroudi, S., Loizou, C., Pantziaris, M., Pattichis, C.: Segmentation of the common carotid intima-media complex in ultrasound images using active contours. IEEE Trans. Biomed. Eng. **59**(11), 3060–3069 (2012)
16. Gupta, R., Pachauri, R., Singh, A.K.: Despeckle and segmentation of carotid artery for measurement of intima-media thickness. In: 2019 International Conference on Signal Processing and Communication (ICSC) (2019)
17. Gupta, R., Pachauri, R., Singh, A.: Linear despeckle approach for ultrasound carotid artery images. J. Intell. Fuzzy Syst. **35**(2), 1807–1816 (2018)
18. Latha, S., Dhanalakshmi, S.: Despeckling of carotid artery ultrasound images with a calculus approach. Curr. Med. Imag. **15**(4), 414–426 (2019)
19. Febin, I.P., Jidesh, P.: Despeckling and enhancement of ultrasound images using non-local variational framework. Vis. Comput. 1–14 (2021)

20. Loizou, C.P., Pattichis, C.S., Pantziaris, M., Nicolaides, A.: An integrated system for the segmentation of atherosclerotic carotid plaque. IEEE Trans. Inf. Technol. Biomed. **11**(6), 661–667 (2007)
21. Loizou, C.P., Pattichis, C.S., Pantziaris, M., Tyllis, T., Nicolaides, A.: Snakes based segmentation of the common carotid artery intima media. Med. Biol. Eng. Comput. **45**, 35–49 (2007)
22. Izquierdo-Zaragoza, J.L., Bastida-Jumilla, M.C., Verdu-Monedero, R., Morales-Sanchez, J., Berenguer-Vidal, R.: Segmentation of the carotid artery in ultrasound images using frequency-designed B-spline active contour. In: 2011 IEEE International Conference on Acoustics, Speech and Signal Processing (ICASSP) (2011)
23. Ramasamy, N., Jayanthi, K.B.: Automated lumen segmentation and estimation of numerical attributes of common carotid artery using longitudinal B-mode ultrasound images. In: 2013 IEEE Point-of-Care Healthcare Technologies (PHT) (2013)
24. Chaudhry, A., Hassan, M., Khan, A., Kim, J.Y.: Automatic active contour-based segmentation and classification of carotid artery ultrasound images. J. Digit. Imaging **26**(6), 1071–1081 (2013)
25. Nagaraj, Y., Madipalli, P., Rajan, J., Kumar, P.K., Narasimhadhan, A.V.: Segmentation of intima media complex from carotid ultrasound images using wind driven optimization technique. Biomed. Signal Process. Control **40**, 462–472 (2018)
26. Latha, S., Samiappan, D., Muthu, P., Kumar, R.: Fully automated integrated segmentation of carotid artery ultrasound images using DBSCAN and affinity propagation. J. Med. Biol. Eng. (2021)
27. Golemati, S., Stoitsis, J., Sifakis, E.G., Balkizas, T., Nikita, K.S.: Using the Hough transform to segment ultrasound images of longitudinal and transverse sections of the carotid artery. Ultrasound Med. Biol. **33**(12), 1918–1932 (2007)
28. Sottile, F., Marino, S., Bramanti, P., Bonanno, L.: Validating a computer-aided diagnosis system for identifying carotid atherosclerosis. In: 2013 6th International Congress on Image and Signal Processing (CISP) (2013)
29. Santos, A.M.F., Tavares, J.M.R.S., Sousa, L., Santos, R., Castro, P., Azevedo, E.: Automatic segmentation of the lumen of the carotid artery in ultrasound B-mode images. In: Medical Imaging 2013: Computer-Aided Diagnosis (2013)
30. Harish Kumar, J.R., Teotia, K., Raj, P.K., Andrade, J., Rajagopal, K.V., Sekhar Seelamantula, C.: Automatic segmentation of common carotid artery in longitudinal mode ultrasound images using active oblongs. In: ICASSP 2019—2019 IEEE International Conference on Acoustics, Speech and Signal Processing (ICASSP) (2019)
31. Dhupia, A., Harish Kumar, J.R., Andrade, J., Rajagopal, K.V.: Automatic segmentation of lumen intima layer in longitudinal mode ultrasound images. In: Annual International Conference of the IEEE Engineering in Medicine and Biology Society, pp. 2125–2128 (2020)
32. Chaudhry, A., Hassan, M., Khan, A., Kim, J.Y., Tuan, T.A.: Automatic segmentation and decision making of carotid artery ultrasound images. In: Advances in Intelligent Systems and Computing, pp. 185–196. Springer Berlin Heidelberg, Berlin (2013)
33. Jin, J., Ding, M., Yang, X.: Automatic detection of the intima-media layer in ultrasound common carotid artery image based on active contour model. In: 2011 International Conference on Intelligent Computation and Bio-Medical Instrumentation (2011)
34. Zhao, S., et al.: Robust segmentation of intima–media borders with different morphologies and dynamics during the cardiac cycle. IEEE J. Biomed. Health Inform. **22**(5), 1571–1582 (2018)
35. Chang, M., Varghese, B., Gunter, J., Lee, K.J., Hwang, D.H., Duddalwar, V.: Feasibility of Nakagami parametric image for texture analysis. In: 15th International Symposium on Medical Information Processing and Analysis (2020)
36. Tsui, P.H., Huang, C.C., Wang, S.H.: Use of Nakagami distribution and logarithmic compression in ultrasonic tissue characterization. J. Med. Biol. Eng. **26**, 69–73 (2006)
37. Destrempes, F., Meunier, J., Giroux, M.-F., Soulez, G., Cloutier, G.: Segmentation in ultrasonic B-mode images of healthy carotid arteries using mixtures of Nakagami distributions and stochastic optimization. IEEE Trans. Med. Imaging **28**(2), 215–229 (2009)

38. Destrempes, F., Meunier, J., Giroux, M.-F., Soulez, G., Cloutier, G.: Segmentation of plaques in sequences of ultrasonic B-mode images of carotid arteries based on motion estimation and a Bayesian model. IEEE Trans. Biomed. Eng. **58**(8), 2202–2211 (2011)
39. Zhou, Y., Cheng, X., Xu, X., Song, E.: Dynamic programming in parallel boundary detection with application to ultrasound intima-media segmentation. Med. Image Anal. **17**(8), 892–906 (2013)
40. Rocha, R., Campilho, A., Silva, J., Azevedo, E., Santos, R.: Segmentation of the carotid intima-media region in B-mode ultrasound images. Image Vis. Comput. **28**(4), 614–625 (2010)
41. Qian, C., Yang, X.: An integrated method for atherosclerotic carotid plaque segmentation in ultrasound image. Comput. Methods Programs Biomed. **153**, 19–32 (2018)
42. Araki, T., et al.: Two automated techniques for carotid lumen diameter measurement: Regional versus boundary approaches. J. Med. Syst. **40**(7), 182 (2016)
43. Lekadir, K., et al.: A convolutional neural network for automatic characterization of plaque composition in carotid ultrasound. IEEE J. Biomed. Health Inform. **21**, 48–55 (2017)
44. Gastounioti, A., Sotiras, A., Nikita, K.S., Paragios, N.: Graph-based motion-driven segmentation of the carotid atherosclerotique plaque in 2D ultrasound sequences. In: Lecture Notes in Computer Science, pp. 551–559. Springer International Publishing, Cham (2015)
45. Hassan, M., Chaudhry, A., Khan, A., Kim, J.Y.: Carotid artery image segmentation using modified spatial fuzzy C-means and ensemble clustering. Comput. Methods Programs Biomed. **108**(3), 1261–1276 (2012)
46. Sumathi, K., Mahesh, V., Ramakrishnan, S.: Analysis of intima media thickness in ultrasound carotid artery images using level set segmentation without re-initialization. In: 2014 International Conference on Informatics, Electronics and Vision (ICIEV) (2014)
47. Lip, G.Y., Rathore, V.S., Katira, R., Watson, R.D., Singh, S.P.: Do Indo-Asians have smaller coronary arteries? Postgrad. Med. J. **75**, 463–466 (1999)
48. Reddy, S., et al.: Coronary artery size in North Indian population—Intravascular ultrasound-based study. Indian Heart J. **71**(5), 412–417 (2019)